

Fully heavy pentaquark states from QCD sum rules

Zheng-Lei Jing and Jian-Rong Zhang

*Department of Physics, College of Science, National University of Defense Technology,
Changsha 410073, Hunan, People's Republic of China*

(Dated: July 23, 2025)

In this work, we systematically investigate the mass spectra of fully heavy pentaquark states $QQQQ\bar{Q}$ within the framework of QCD sum rules. Employing three configurations of interpolating currents, we obtain the following mass predictions: for the $cccc\bar{c}$ states, the masses are determined to be $7.79_{-0.17}^{+0.18}$ GeV, $7.76_{-0.18}^{+0.23}$ GeV, $7.81_{-0.18}^{+0.17}$ GeV; while for the $bbbb\bar{b}$ states, the corresponding masses are calculated as $22.35_{-0.19}^{+0.19}$ GeV, $22.27_{-0.22}^{+0.22}$ GeV, $22.37_{-0.20}^{+0.18}$ GeV, respectively.

PACS numbers: 11.55.Hx, 12.38.Lg, 12.39.Mk

I. INTRODUCTION

Hadron physics represents a pivotal frontier in contemporary particle physics research, primarily investigating bound states of quarks and gluons governed by strong interactions. Conventionally, hadronic states are categorized into two fundamental types: mesons and baryons. However, quantum chromodynamics (QCD) imposes no fundamental constraints limiting hadrons to conventional configurations. The theory naturally accommodates more complex structures, including multi-quark systems and gluonic bound states, which are collectively termed exotic hadrons. Currently, the exploration of exotic hadron states stands as one of the most significant and active research domains within hadron physics. One could see some recent reviews [1–9] and references therein.

The investigation of exotic hadron states gained significant promotion with the discovery of the $X(3872)$ resonance [10]. Observed by the decay channel $B^\pm \rightarrow K^\pm \pi^+ \pi^- J/\psi$, this state displayed characteristics that challenged conventional quark model predictions. Its unusual properties stimulated intense theoretical and experimental scrutiny of exotic hadronic matter, including observations of pentaquark states with the discovery of the $P_c(4380)^+$ and $P_c(4450)^+$ resonances by the LHCb Collaboration in the $\Lambda_b^0 \rightarrow J/\psi p K^-$ decay channel [11]. Subsequent analysis with improved statistics in 2019 revealed a new state, $P_c(4312)^+$, while resolving the broad $P_c(4450)^+$ peak into two narrow structures, $P_c(4440)^+$ and $P_c(4457)^+$ [12]. The LHCb Collaboration has further reported two additional observations: the $P_{cs}(4459)^0$ state, identified in the $J/\psi \Lambda$ mass spectrum of $\Xi_b^- \rightarrow J/\psi \Lambda K^-$ decays [13], and the $P_{cs}(4338)^0$ state, found through amplitude analysis of $B^- \rightarrow J/\psi \Lambda \bar{p}$ decays [14]. Moreover, the $P_c(4337)^+$ state observed by LHCb in $B_s^0 \rightarrow J/\psi p \bar{p}$ decays has been considered to be a promising pentaquark state candidate [15]. In 2020, the LHCb Collaboration reported a narrow structure $X(6900)$ and proposed it to be a all-charmed tetraquark state [16], which has greatly stimulated the study of fully heavy multi-quark states.

On investigations of fully heavy pentaquark states, researchers have employed a variety of theoretical methodologies [17–31]. Concretely, studies have been conducted within the chromomagnetic interaction model [17], chiral quark model [20, 24], Lattice-QCD inspired quark model [22], MIT bag model [23], and nonrelativistic potential quark model [25]. In addition, analyses of fully heavy pentaquark states have been carried out utilizing approaches such as the variational method within the constituent quark model [21], the diffusion Monte Carlo method [27], the Suzuki model [29], and the extended form of the Gursej-Radicati mass formula [30].

During the study of fully heavy pentaquark states, it is inevitably to confront the highly intricate nonperturbative problems inherent in QCD. As one reliable method for evaluating nonperturbative effects, the QCD sum rule [32, 33] is firmly established on the basic QCD theory and has been successfully used in the study of hadronic states [34–38]. By far, some works have made use of QCD sum rules to address the nonperturbative issues on fully heavy pentaquark states [18, 19, 26, 28]. In Ref. [18], the author gained a mass of $7.41_{-0.21}^{+0.27}$ GeV for $cccc\bar{c}$ states and $21.60_{-0.22}^{+0.73}$ GeV for $bbbb\bar{b}$ states, suggesting that these states could be observed in the $\Omega_{QQQ}\eta_Q$ invariant mass spectrum. Ref. [19] focused on the diquark-diquark-antiquark type fully heavy pentaquark states with the spin-parity $J^P = \frac{1}{2}^-$, obtaining the mass of $cccc\bar{c}$ to be 7.93 ± 0.15 GeV and that of $bbbb\bar{b}$ to be 23.91 ± 0.15 GeV. The author proposed that these states might be detectable in the $J/\psi\Omega_{ccc}$ and $\Upsilon\Omega_{bbb}$ invariant mass spectrum. Ref. [26] researched the full-charm and full-bottom pentaquark states with spin-parity $\frac{3}{2}^-$, reporting masses of 7628 ± 112 MeV and 21982 ± 144 MeV, respectively. In Ref. [28], the authors analyzed the fully heavy pentaquark candidates with quark contents of $ccb\bar{c}$ and $bbb\bar{c}$. For the P_{4cb} states, they obtained masses of 11388.30 ± 107.79 MeV and 11368.30 ± 112.68 MeV, while for P_{4bc} states, the reported masses were 20998.30 ± 121.52 MeV and 20990.50 ± 125.87 MeV.

In this paper, we devote to extend our previous research [18] and systematically investigate the fully heavy pentaquark states from QCD sum rules. The remainder of the paper is organized as follows: the derivation of the QCD sum rules for fully heavy pentaquark states is presented in section II, and the numerical analysis and discussions are given in section III. The final section comprises a concise summary.

II. FULLY HEAVY PENTAQUARK STATES IN QCD SUM RULES

Based on the interpolating current construction ways for heavy mesons [39] and baryons [40, 41] in full QCD, we can formulate following forms of currents

$$j_\mu = (\epsilon_{abc} Q_a^T C \gamma_\mu Q_b Q_c)(Q_e \bar{Q}_e), \quad (1)$$

$$j_{\mu\rho} = (\epsilon_{abc} Q_a^T C \gamma_\mu Q_b Q_c)(Q_e \gamma_\rho \bar{Q}_e), \quad (2)$$

and

$$j_{\mu\rho} = (\epsilon_{abc} Q_a^T C \gamma_\mu Q_b Q_c)(Q_e \gamma_\rho \gamma_5 \bar{Q}_e) \quad (3)$$

for $QQQQ\bar{Q}$ pentaquark states. Here, T denotes the transpose of a matrix, C denotes the charge conjugate matrix, and Q can be either a heavy charm or bottom quark. The subscripts $a, b, c,$ and e are colour indices.

In order to derive the QCD sum rule, one can construct the two-point correlator

$$\Pi_{\mu\nu}(q^2) = i \int d^4x e^{iq \cdot x} \langle 0 | T [j_\mu(x) \bar{j}_\nu(0)] | 0 \rangle \quad (4)$$

for the current in Eq. (1). The parameterization of $\Pi_{\mu\nu}(q^2)$ is as follows

$$\Pi_{\mu\nu}(q^2) = -g_{\mu\nu} [q\Pi_1(q^2) + \Pi_2(q^2)] + \dots \quad (5)$$

For the currents in Eq. (2) and Eq. (3), the two-point correlator

$$\Pi_{\mu\rho\nu\sigma}(q^2) = i \int d^4x e^{iq \cdot x} \langle 0 | T [j_{\mu\rho}(x) \bar{j}_{\nu\sigma}(0)] | 0 \rangle \quad (6)$$

can be parameterized as

$$\Pi_{\mu\rho\nu\sigma}(q^2) = -g_{\mu\nu}g_{\rho\sigma} [\not{q}\Pi_1(q^2) + \Pi_2(q^2)] + \dots \quad (7)$$

By matching the terms proportional to $-g_{\mu\nu}\not{q}$ or $-g_{\mu\nu}g_{\rho\sigma}\not{q}$ in the hadronic representation with the quark representation and after applying the Borel transform, one gets

$$\lambda^2 e^{-M_H^2/M^2} = \int_{25m_Q^2}^{s_0} ds \rho e^{-s/M^2}, \quad (8)$$

where M_H is the mass of the studied hadron and the spectral density is $\rho = \frac{1}{\pi}\text{Im}\Pi_1(s)$. The hadron mass is obtained by taking the derivative of Eq. (8) with respect to $-\frac{1}{M^2}$ and dividing by Eq. (8) itself. The expression is

$$M_H = \sqrt{\int_{25m_Q^2}^{s_0} ds \rho s e^{-s/M^2} / \int_{25m_Q^2}^{s_0} ds \rho e^{-s/M^2}}. \quad (9)$$

In OPE calculations, one usually employs heavy quark propagators in momentum space [39]. By extending the relevant techniques [42–48] to fully heavy pentaquark systems as Ref. [18], the specific expression for the spectral density $\rho = \rho^{\text{pert}} + \rho^{\langle g^2 G^2 \rangle} + \rho^{\langle g^3 G^3 \rangle}$ in Eq. (9) is calculated to be

$$\begin{aligned} \rho^{\text{pert}} &= -\frac{3}{5 \times 2^{14} \pi^8} \int_{\alpha_{\min}}^{\alpha_{\max}} \frac{d\alpha}{\alpha^3} \int_{\beta_{\min}}^{\beta_{\max}} \frac{d\beta}{\beta^3} \int_{\gamma_{\min}}^{\gamma_{\max}} \frac{d\gamma}{\gamma^3} \int_{\xi_{\min}}^{\xi_{\max}} \frac{d\xi}{\xi^3} \frac{\mathbf{h}^3 (m_Q^2 - \mathbf{h}s)^3}{(1 - \alpha - \beta - \gamma - \xi)^3} \left\{ 8\mathbf{h}^2 (m_Q^2 - \mathbf{h}s)^2 \right. \\ &\quad \left. - [35\mathbf{h}^3 s + 5\mathbf{h}m_Q^2(3\alpha\beta - 2\gamma\xi)] (m_Q^2 - \mathbf{h}s) + 20\mathbf{h}^4 s^2 + 20\mathbf{h}^2 s m_Q^2 (\alpha\beta - \gamma\xi) - 20\alpha\beta\gamma\xi m_Q^4 \right\}, \\ \rho^{\langle g^2 G^2 \rangle} &= -\frac{m_Q^2 \langle g^2 G^2 \rangle}{2^{14} \pi^8} \int_{\alpha_{\min}}^{\alpha_{\max}} \frac{d\alpha}{\alpha^3} \int_{\beta_{\min}}^{\beta_{\max}} \frac{d\beta}{\beta^3} \int_{\gamma_{\min}}^{\gamma_{\max}} \frac{d\gamma}{\gamma^3} \int_{\xi_{\min}}^{\xi_{\max}} \frac{d\xi}{\xi^3} \frac{\mathbf{h}^3}{(1 - \alpha - \beta - \gamma - \xi)^3} \left\{ [(1 - \alpha - \beta - \gamma - \xi)^3 \right. \\ &\quad + 2\beta^3 + 2\xi^3] [4\mathbf{h}^2 (m_Q^2 - \mathbf{h}s)^2 - 7\mathbf{h}^3 s (m_Q^2 - \mathbf{h}s) + \mathbf{h}^4 s^2 - \alpha\beta\gamma\xi m_Q^4 - \mathbf{h}m_Q^2 (3\alpha\beta - 2\gamma\xi) (m_Q^2 - \mathbf{h}s) \\ &\quad + \mathbf{h}^2 s m_Q^2 (\alpha\beta - \gamma\xi)] + 3\mathbf{h} (2\gamma\xi^3 - 3\alpha\beta^3) (m_Q^2 - \mathbf{h}s)^2 - 6(\gamma\xi^3 - \alpha\beta^3) \mathbf{h}^2 s (m_Q^2 - \mathbf{h}s) \\ &\quad \left. - 6\alpha\beta\gamma\xi (\beta^2 + \xi^2) m_Q^2 (m_Q^2 - \mathbf{h}s) \right\}, \end{aligned}$$

and

$$\begin{aligned} \rho^{\langle g^3 G^3 \rangle} &= -\frac{\langle g^3 G^3 \rangle}{2^{16} \pi^8} \int_{\alpha_{\min}}^{\alpha_{\max}} \frac{d\alpha}{\alpha^3} \int_{\beta_{\min}}^{\beta_{\max}} \frac{d\beta}{\beta^3} \int_{\gamma_{\min}}^{\gamma_{\max}} \frac{d\gamma}{\gamma^3} \int_{\xi_{\min}}^{\xi_{\max}} \frac{d\xi}{\xi^3} \frac{\mathbf{h}^3}{(1 - \alpha - \beta - \gamma - \xi)^3} \left\{ [(1 - \alpha - \beta - \gamma - \xi)^3 + 2\beta^3 + 2\xi^3] \right. \\ &\quad [4\mathbf{h}^2 (m_Q^2 - \mathbf{h}s)^2 - 7\mathbf{h}^3 s (m_Q^2 - \mathbf{h}s) + \mathbf{h}^4 s^2] - \alpha\beta\gamma\xi m_Q^4 [(1 - \alpha - \beta - \gamma - \xi)^3 + 12\beta^3 + 12\xi^3] \\ &\quad - \mathbf{h}\alpha\beta m_Q^2 [(1 - \alpha - \beta - \gamma - \xi)^3 + 12\beta^3 + 2\xi^3] (3m_Q^2 - 4\mathbf{h}s) + \mathbf{h}\gamma\xi m_Q^2 [(1 - \alpha - \beta - \gamma - \xi)^3 + 2\beta^3 + 12\xi^3] \\ &\quad \left. \times (2m_Q^2 - 3\mathbf{h}s) + 2[(1 - \alpha - \beta - \gamma - \xi)^4 + 2\beta^4 + 2\xi^4] [\mathbf{h}^2 m_Q^2 (8m_Q^2 - 15\mathbf{h}s) + \mathbf{h}m_Q^4 (2\gamma\xi - 3\alpha\beta)] \right\} \end{aligned}$$

for the current (1),

$$\begin{aligned} \rho^{\text{pert}} &= \frac{3}{2^{14} \pi^8} \int_{\alpha_{\min}}^{\alpha_{\max}} \frac{d\alpha}{\alpha^3} \int_{\beta_{\min}}^{\beta_{\max}} \frac{d\beta}{\beta^3} \int_{\gamma_{\min}}^{\gamma_{\max}} \frac{d\gamma}{\gamma^3} \int_{\xi_{\min}}^{\xi_{\max}} \frac{d\xi}{\xi^3} \frac{\mathbf{h}^3 (m_Q^2 - \mathbf{h}s)^3}{(1 - \alpha - \beta - \gamma - \xi)^3} \left\{ \mathbf{h}^2 (m_Q^2 - \mathbf{h}s)^2 \right. \\ &\quad \left. - [6\mathbf{h}^3 s + 2\mathbf{h}m_Q^2 (\alpha\beta + \gamma\xi)] (m_Q^2 - \mathbf{h}s) + 4\mathbf{h}^4 s^2 + 4\mathbf{h}^2 s m_Q^2 (\alpha\beta + \gamma\xi) + 4\alpha\beta\gamma\xi m_Q^4 \right\}, \end{aligned}$$

$$\begin{aligned} \rho\langle g^2 G^2 \rangle &= \frac{m_Q^2 \langle g^2 G^2 \rangle}{2^{15} \pi^8} \int_{\alpha_{\min}}^{\alpha_{\max}} \frac{d\alpha}{\alpha^3} \int_{\beta_{\min}}^{\beta_{\max}} \frac{d\beta}{\beta^3} \int_{\gamma_{\min}}^{\gamma_{\max}} \frac{d\gamma}{\gamma^3} \int_{\xi_{\min}}^{\xi_{\max}} \frac{d\xi}{\xi^3} \frac{\mathbf{h}^3}{(1-\alpha-\beta-\gamma-\xi)^3} \left\{ \left[(1-\alpha-\beta-\gamma-\xi)^3 \right. \right. \\ &+ 2\beta^3 + 2\xi^3 \left. \right] \left[5\mathbf{h}^2(m_Q^2 - \mathbf{h}s)^2 - 12\mathbf{h}^3 s(m_Q^2 - \mathbf{h}s) + 2\mathbf{h}^4 s^2 + 2\alpha\beta\gamma\xi m_Q^4 - 4\mathbf{h}m_Q^2(\alpha\beta + \gamma\xi)(m_Q^2 - \mathbf{h}s) \right. \\ &+ 2\mathbf{h}^2 s m_Q^2(\alpha\beta + \gamma\xi) \left. \right] - 12\mathbf{h}(\gamma\xi^3 + \alpha\beta^3)(m_Q^2 - \mathbf{h}s)^2 + 12(\gamma\xi^3 + \alpha\beta^3)\mathbf{h}^2 s(m_Q^2 - \mathbf{h}s) \\ &\left. \left. + 12\alpha\beta\gamma\xi(\beta^2 + \xi^2)m_Q^2(m_Q^2 - \mathbf{h}s) \right\}, \end{aligned}$$

and

$$\begin{aligned} \rho\langle g^3 G^3 \rangle &= \frac{\langle g^3 G^3 \rangle}{2^{17} \pi^8} \int_{\alpha_{\min}}^{\alpha_{\max}} \frac{d\alpha}{\alpha^3} \int_{\beta_{\min}}^{\beta_{\max}} \frac{d\beta}{\beta^3} \int_{\gamma_{\min}}^{\gamma_{\max}} \frac{d\gamma}{\gamma^3} \int_{\xi_{\min}}^{\xi_{\max}} \frac{d\xi}{\xi^3} \frac{\mathbf{h}^3}{(1-\alpha-\beta-\gamma-\xi)^3} \left\{ \left[(1-\alpha-\beta-\gamma-\xi)^3 + 2\beta^3 + 2\xi^3 \right] \right. \\ &\left[5\mathbf{h}^2(m_Q^2 - \mathbf{h}s)^2 - 12\mathbf{h}^3 s(m_Q^2 - \mathbf{h}s) + 2\mathbf{h}^4 s^2 \right] + 2\alpha\beta\gamma\xi m_Q^4 \left[(1-\alpha-\beta-\gamma-\xi)^3 + 12\beta^3 + 12\xi^3 \right] \\ &- \mathbf{h}\alpha\beta m_Q^2 \left[(1-\alpha-\beta-\gamma-\xi)^3 + 12\beta^3 + 2\xi^3 \right] (4m_Q^2 - 6\mathbf{h}s) - \mathbf{h}\gamma\xi m_Q^2 \left[(1-\alpha-\beta-\gamma-\xi)^3 + 2\beta^3 + 12\xi^3 \right] \\ &\left. \times (4m_Q^2 - 6\mathbf{h}s) + 2 \left[(1-\alpha-\beta-\gamma-\xi)^4 + 2\beta^4 + 2\xi^4 \right] \left[\mathbf{h}^2 m_Q^2 (10m_Q^2 - 22\mathbf{h}s) + 4\mathbf{h}m_Q^4(\gamma\xi + \alpha\beta) \right] \right\} \end{aligned}$$

for the current (2), as well as

$$\begin{aligned} \rho^{\text{pert}} &= -\frac{3}{2^{14} \pi^8} \int_{\alpha_{\min}}^{\alpha_{\max}} \frac{d\alpha}{\alpha^3} \int_{\beta_{\min}}^{\beta_{\max}} \frac{d\beta}{\beta^3} \int_{\gamma_{\min}}^{\gamma_{\max}} \frac{d\gamma}{\gamma^3} \int_{\xi_{\min}}^{\xi_{\max}} \frac{d\xi}{\xi^3} \frac{\mathbf{h}^3(m_Q^2 - \mathbf{h}s)^3}{(1-\alpha-\beta-\gamma-\xi)^3} \left\{ \mathbf{h}^2(m_Q^2 - \mathbf{h}s)^2 \right. \\ &\left. - [6\mathbf{h}^3 s + 2\mathbf{h}m_Q^2(\alpha\beta - \gamma\xi)](m_Q^2 - \mathbf{h}s) + 4\mathbf{h}^4 s^2 + 4\mathbf{h}^2 s m_Q^2(\alpha\beta - \gamma\xi) - 4\alpha\beta\gamma\xi m_Q^4 \right\}, \end{aligned}$$

$$\begin{aligned} \rho\langle g^2 G^2 \rangle &= -\frac{m_Q^2 \langle g^2 G^2 \rangle}{2^{15} \pi^8} \int_{\alpha_{\min}}^{\alpha_{\max}} \frac{d\alpha}{\alpha^3} \int_{\beta_{\min}}^{\beta_{\max}} \frac{d\beta}{\beta^3} \int_{\gamma_{\min}}^{\gamma_{\max}} \frac{d\gamma}{\gamma^3} \int_{\xi_{\min}}^{\xi_{\max}} \frac{d\xi}{\xi^3} \frac{\mathbf{h}^3}{(1-\alpha-\beta-\gamma-\xi)^3} \left\{ \left[(1-\alpha-\beta-\gamma-\xi)^3 \right. \right. \\ &+ 2\beta^3 + 2\xi^3 \left. \right] \left[5\mathbf{h}^2(m_Q^2 - \mathbf{h}s)^2 - 12\mathbf{h}^3 s(m_Q^2 - \mathbf{h}s) + 2\mathbf{h}^4 s^2 - 2\alpha\beta\gamma\xi m_Q^4 - 4\mathbf{h}m_Q^2(\alpha\beta - \gamma\xi)(m_Q^2 - \mathbf{h}s) \right. \\ &+ 2\mathbf{h}^2 s m_Q^2(\alpha\beta - \gamma\xi) \left. \right] + 12\mathbf{h}(\gamma\xi^3 - \alpha\beta^3)(m_Q^2 - \mathbf{h}s)^2 - 12(\gamma\xi^3 - \alpha\beta^3)\mathbf{h}^2 s(m_Q^2 - \mathbf{h}s) \\ &\left. \left. - 12\alpha\beta\gamma\xi(\beta^2 + \xi^2)m_Q^2(m_Q^2 - \mathbf{h}s) \right\}, \end{aligned}$$

and

$$\begin{aligned} \rho\langle g^3 G^3 \rangle &= -\frac{\langle g^3 G^3 \rangle}{2^{17} \pi^8} \int_{\alpha_{\min}}^{\alpha_{\max}} \frac{d\alpha}{\alpha^3} \int_{\beta_{\min}}^{\beta_{\max}} \frac{d\beta}{\beta^3} \int_{\gamma_{\min}}^{\gamma_{\max}} \frac{d\gamma}{\gamma^3} \int_{\xi_{\min}}^{\xi_{\max}} \frac{d\xi}{\xi^3} \frac{\mathbf{h}^3}{(1-\alpha-\beta-\gamma-\xi)^3} \left\{ \left[(1-\alpha-\beta-\gamma-\xi)^3 + 2\beta^3 + 2\xi^3 \right] \right. \\ &\left[5\mathbf{h}^2(m_Q^2 - \mathbf{h}s)^2 - 12\mathbf{h}^3 s(m_Q^2 - \mathbf{h}s) + 2\mathbf{h}^4 s^2 \right] - 2\alpha\beta\gamma\xi m_Q^4 \left[(1-\alpha-\beta-\gamma-\xi)^3 + 12\beta^3 + 12\xi^3 \right] \\ &- \mathbf{h}\alpha\beta m_Q^2 \left[(1-\alpha-\beta-\gamma-\xi)^3 + 12\beta^3 + 2\xi^3 \right] (4m_Q^2 - 6\mathbf{h}s) + \mathbf{h}\gamma\xi m_Q^2 \left[(1-\alpha-\beta-\gamma-\xi)^3 + 2\beta^3 + 12\xi^3 \right] \\ &\left. \times (4m_Q^2 - 6\mathbf{h}s) + 2 \left[(1-\alpha-\beta-\gamma-\xi)^4 + 2\beta^4 + 2\xi^4 \right] \left[\mathbf{h}^2 m_Q^2 (10m_Q^2 - 22\mathbf{h}s) - 4\mathbf{h}m_Q^4(\gamma\xi - \alpha\beta) \right] \right\} \end{aligned}$$

for the current (3).

It is defined as $\mathbf{h} = \frac{1}{\frac{1}{\alpha} + \frac{1}{\beta} + \frac{1}{\gamma} + \frac{1}{\xi} + \frac{1}{1-\alpha-\beta-\gamma-\xi}}$, and the integration limits of α, β, γ , and ξ are

given by

$$\alpha = \frac{1}{2} \left[\left(1 - \frac{15m_Q^2}{s} \right) \pm \sqrt{\left(1 - \frac{15m_Q^2}{s} \right)^2 - \frac{4m_Q^2}{s}} \right],$$

$$\beta = \frac{1}{2} \left[\left(1 - \alpha - \frac{8\alpha m_Q^2}{\alpha s - m_Q^2} \right) \pm \sqrt{\left(1 - \alpha - \frac{8\alpha m_Q^2}{\alpha s - m_Q^2} \right)^2 - \frac{4\alpha(1-\alpha)m_Q^2}{\alpha s - m_Q^2}} \right],$$

$$\gamma = \frac{1}{2} \left[\left(1 - \alpha - \beta - \frac{3}{\frac{s}{m_Q^2} - \frac{1}{\alpha} - \frac{1}{\beta}} \right) \pm \sqrt{\left(1 - \alpha - \beta - \frac{3}{\frac{s}{m_Q^2} - \frac{1}{\alpha} - \frac{1}{\beta}} \right)^2 - 4 \frac{1 - \alpha - \beta}{\frac{s}{m_Q^2} - \frac{1}{\alpha} - \frac{1}{\beta}}} \right],$$

and

$$\xi = \frac{1}{2} \left[(1 - \alpha - \beta - \gamma) \pm \sqrt{(1 - \alpha - \beta - \gamma)^2 - 4 \frac{1 - \alpha - \beta - \gamma}{\frac{s}{m_Q^2} - \frac{1}{\alpha} - \frac{1}{\beta} - \frac{1}{\gamma}}} \right].$$

III. NUMERICAL ANALYSIS AND DISCUSSIONS

In QCD sum rules, one expands the correlation function by perturbation and non perturbation approximation in the OPE calculation, and introduces a complex dispersion integral structure including hadronic resonance and continuous spectrum at the phenomenological level. In order to reliably extract the information of hadronic resonance states, it is necessary to determine the appropriate working windows of the continuum threshold $\sqrt{s_0}$ and the Borel parameter M^2 . The threshold $\sqrt{s_0}$ represents the starting energy point of the continuum state, and the energy gap $\sqrt{s_0} - M_H$ is typically estimated at approximately 0.3 – 0.8 GeV [49]. The Borel parameter is determined from two considerations. First, the lower bound is determined by the convergence requirement of the OPE, ensuring that higher-order term contributions can be safely neglected. Second, the upper bound is constrained by the condition that pole contribution should significantly exceed continuum contribution.

The input parameters are taken as $\langle g^2 G^2 \rangle = 0.88 \pm 0.25 \text{ GeV}^4$, $\langle g^3 G^3 \rangle = 0.58 \pm 0.18 \text{ GeV}^6$ [32, 33, 49–53] and m_Q is set to the running charm mass $m_c = 1.2730 \pm 0.0046 \text{ GeV}$ [54]. For the $cccc\bar{c}$ represented by the current (1), based on the typical energy gap characteristics between the continuum spectrum and the resonance state, $\sqrt{s_0}$ takes the value in the range of 8.0 – 8.4 GeV. The lower limit of the Borel parameter is taken to be $M^2 \geq 3.5 \text{ GeV}^2$. The pole relative contribution at $\sqrt{s_0} = 8.2 \text{ GeV}$ reaches a critical value of 50% at $M^2 = 4.1 \text{ GeV}^2$, and this contribution decreases monotonically with increasing M^2 . Based on the pole dominance condition, the choice of the Borel window at $\sqrt{s_0} = 8.2 \text{ GeV}$ is finalized as $M^2 \in [3.5, 4.1] \text{ GeV}^2$. By analyzing the pole dominance of the system and the OPE convergence test, it can be obtained that when $\sqrt{s_0} = 8.0 \text{ GeV}$, the corresponding Borel window is $M^2 \in [3.5, 3.6] \text{ GeV}^2$; while when $\sqrt{s_0}$ increases to 8.4 GeV, the Borel window extends to $M^2 \in [3.5, 4.5] \text{ GeV}^2$ accordingly.

In the calculations, the parameters are kept at their center values. The Borel curves for the $cccc\bar{c}$ pentaquark states are shown in Fig. 1, Fig. 2, and Fig. 3. The extracted masses of bound

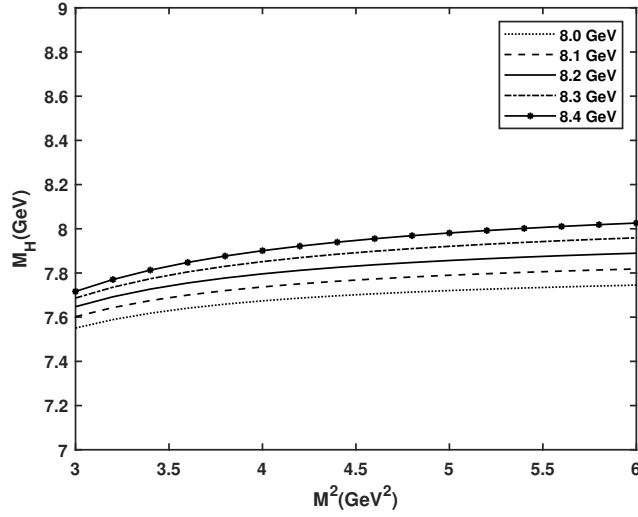


Figure 1: The Borel Curves for $cccc\bar{c}$ state of current (1). The Borel windows of M^2 are $3.5\text{--}3.6\text{ GeV}^2$ for $\sqrt{s_0} = 8.0\text{ GeV}$, $3.5\text{--}4.1\text{ GeV}^2$ for $\sqrt{s_0} = 8.2\text{ GeV}$, and $3.5\text{--}4.5\text{ GeV}^2$ for $\sqrt{s_0} = 8.4\text{ GeV}$, respectively.

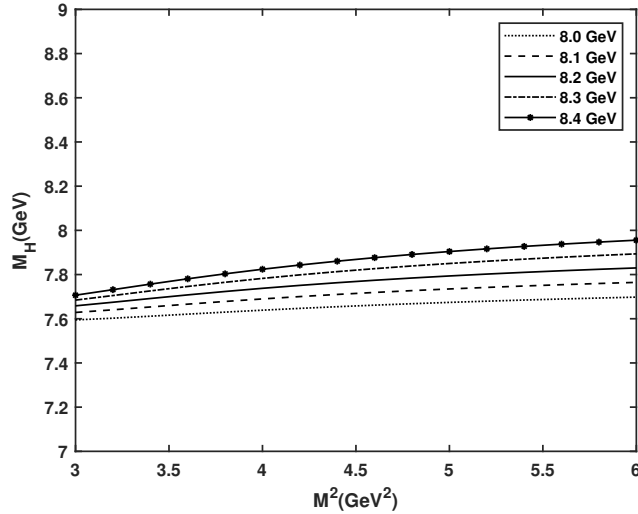


Figure 2: The Borel Curves for $cccc\bar{c}$ state of current (2). The Borel windows of M^2 are $3.5\text{--}3.7\text{ GeV}^2$ for $\sqrt{s_0} = 8.0\text{ GeV}$, $3.5\text{--}4.4\text{ GeV}^2$ for $\sqrt{s_0} = 8.2\text{ GeV}$, and $3.5\text{--}5.1\text{ GeV}^2$ for $\sqrt{s_0} = 8.4\text{ GeV}$, respectively.

states within the optimally chosen working windows are $M_{H1} = 7.79^{+0.16}_{-0.16}\text{ GeV}$ for current (1), $M_{H2} = 7.76^{+0.18}_{-0.15}\text{ GeV}$ for current (2), and $M_{H3} = 7.81^{+0.15}_{-0.17}\text{ GeV}$ for current (3). After systematically accounting for uncertainties in the input parameters, the extracted masses of the $cccc\bar{c}$ pentaquark states are $M_{H1} = 7.79^{+0.16+0.02}_{-0.16-0.01}\text{ GeV}$, $M_{H2} = 7.76^{+0.18+0.05}_{-0.15-0.03}\text{ GeV}$, as well as $M_{H3} = 7.81^{+0.15+0.02}_{-0.17-0.01}\text{ GeV}$. The first uncertainty arises from the variation in the value of the continuous threshold parameter $\sqrt{s_0}$, while the second arises from the errors in the QCD parameters. These results can also be expressed concisely as $M_{H1} = 7.79^{+0.18}_{-0.17}\text{ GeV}$, $M_{H2} = 7.76^{+0.23}_{-0.18}\text{ GeV}$, and $M_{H3} = 7.81^{+0.17}_{-0.18}\text{ GeV}$.

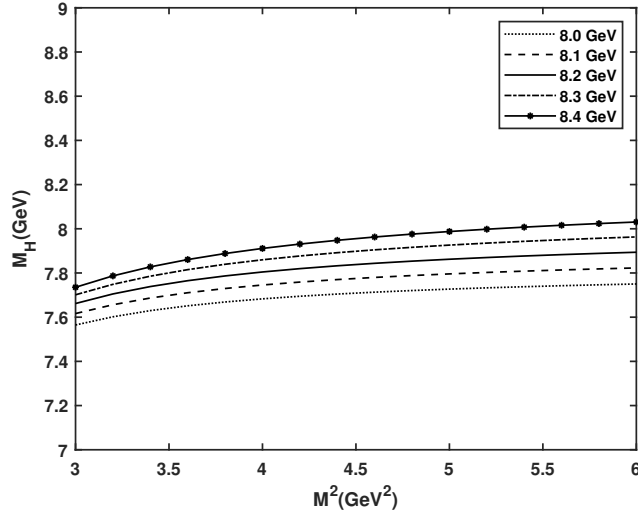


Figure 3: The Borel Curves for $cccc\bar{c}$ state of current (3). The Borel windows of M^2 are $3.5\text{--}3.6\text{ GeV}^2$ for $\sqrt{s_0} = 8.0\text{ GeV}$, $3.5\text{--}3.9\text{ GeV}^2$ for $\sqrt{s_0} = 8.2\text{ GeV}$, and $3.5\text{--}4.5\text{ GeV}^2$ for $\sqrt{s_0} = 8.4\text{ GeV}$, respectively.

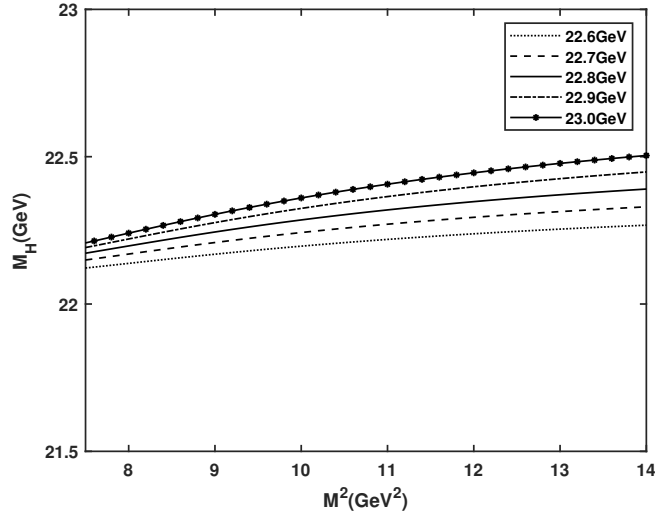


Figure 4: The Borel Curves for $bbbb\bar{b}$ state of current (1). The Borel windows of M^2 are $8\text{--}10.6\text{ GeV}^2$ for $\sqrt{s_0} = 22.6\text{ GeV}$, $8.0\text{--}12.3\text{ GeV}^2$ for $\sqrt{s_0} = 22.8\text{ GeV}$, and $8.0\text{--}13.7\text{ GeV}^2$ for $\sqrt{s_0} = 23.0\text{ GeV}$, respectively.

For the systematic analysis of the fully bottomed $bbbb\bar{b}$ pentaquark states, we use the running bottom quark mass $m_b = 4.183 \pm 0.007\text{ GeV}$ [54] instead of the mass m_c . The threshold $\sqrt{s_0}$ range for the $bbbb\bar{b}$ state is taken as $22.6\text{--}23.0\text{ GeV}$, and the Borel curves are shown in Fig. 4, Fig. 5, and Fig. 6. The final calculated masses of the $bbbb\bar{b}$ states are $M_{H1} = 22.35^{+0.17+0.02}_{-0.11-0.08}\text{ GeV}$, $M_{H2} = 22.27^{+0.20+0.02}_{-0.15-0.07}\text{ GeV}$, and $M_{H3} = 22.37^{+0.15+0.03}_{-0.13-0.07}\text{ GeV}$. These results can also be briefly written as $M_{H1} = 22.35^{+0.19}_{-0.19}\text{ GeV}$, $M_{H2} = 22.27^{+0.22}_{-0.22}\text{ GeV}$, and $M_{H3} = 22.37^{+0.18}_{-0.20}\text{ GeV}$. In Table I, we collect our final results for the mass spectra of fully heavy pentaquark states and compare with other works.

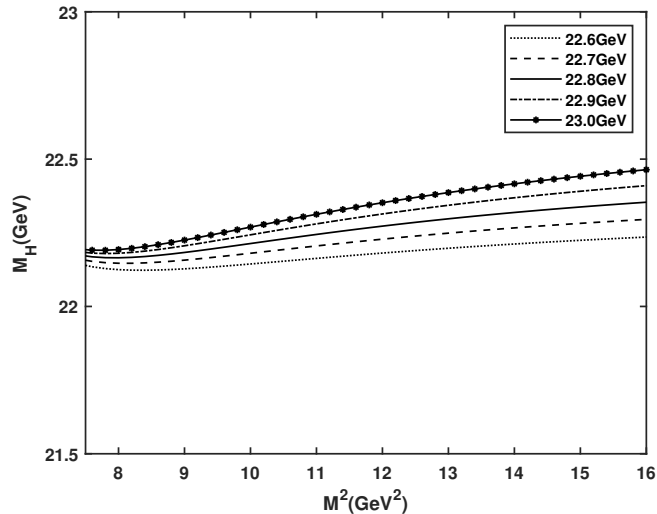


Figure 5: The Borel Curves for $bbb\bar{b}$ state of current (2). The Borel windows of M^2 are 8–12.6 GeV^2 for $\sqrt{s_0} = 22.6$ GeV, 8.0 – 14.3 GeV^2 for $\sqrt{s_0} = 22.8$ GeV, and 8.0 – 16.0 GeV^2 for $\sqrt{s_0} = 23.0$ GeV, respectively.

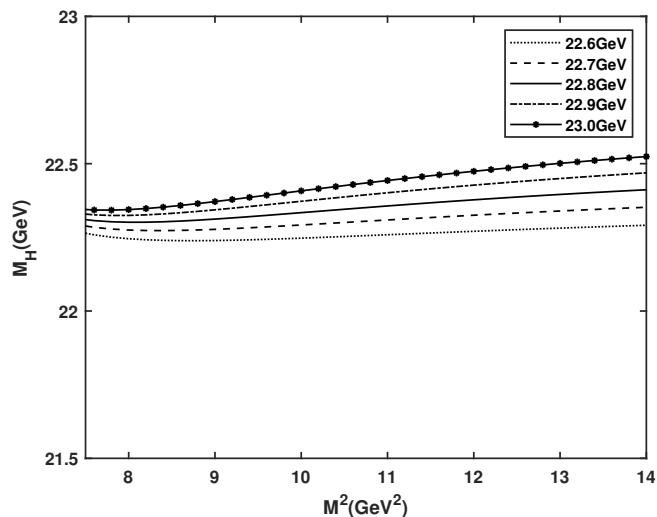


Figure 6: The Borel Curves for $bbb\bar{b}$ state of current (3). The Borel windows of M^2 are 8–10.6 GeV^2 for $\sqrt{s_0} = 22.6$ GeV, 8.0 – 12.2 GeV^2 for $\sqrt{s_0} = 22.8$ GeV, and 8.0 – 13.7 GeV^2 for $\sqrt{s_0} = 23.0$ GeV, respectively.

IV. SUMMARY

In the framework of QCD sum rule method, we have systematically studied fully heavy pentaquark $QQQQ\bar{Q}$ states and finally obtained their mass spectra. For three different configurations of currents, the corresponding masses are presented as $7.79_{-0.17}^{+0.18}$ GeV, $7.76_{-0.18}^{+0.23}$ GeV, $7.81_{-0.18}^{+0.17}$ GeV for the $cccc\bar{c}$ states, and $22.35_{-0.19}^{+0.19}$ GeV, $22.27_{-0.22}^{+0.22}$ GeV, $22.37_{-0.20}^{+0.18}$ GeV for the $bbb\bar{b}$ states, respectively. These fully heavy pentaquark states might be experimentally searched for in strong decay channels,

Table I: The mass spectra of fully heavy pentaquark states (mass in unit of MeV except for “Our works”)

$QQQQ\bar{Q}$	Configurations of the currents	J^P	Our works (GeV)	Ref. [17]	Ref. [21]	Ref. [26]
$cccc\bar{c}$	$(\epsilon_{abc} Q_a^T C \gamma_\mu Q_b Q_c)(Q_e i \gamma_5 \bar{Q}_e)$	$\frac{3}{2}^-$	$7.41_{-0.31}^{+0.27}$ [18]	7864	8144.6	7628 ± 112
$bbbb\bar{b}$	$(\epsilon_{abc} Q_a^T C \gamma_\mu Q_b Q_c)(Q_e i \gamma_5 \bar{Q}_e)$	$\frac{3}{2}^-$	$21.60_{-0.22}^{+0.73}$ [18]	23775	24210.9	21982 ± 144
$cccc\bar{c}$	$(\epsilon_{abc} Q_a^T C \gamma_\mu Q_b Q_c)(Q_e \bar{Q}_e)$	$\frac{3}{2}^+$	$7.79_{-0.17}^{+0.18}$			
$bbbb\bar{b}$	$(\epsilon_{abc} Q_a^T C \gamma_\mu Q_b Q_c)(Q_e \bar{Q}_e)$	$\frac{3}{2}^+$	$22.35_{-0.19}^{+0.19}$			
$cccc\bar{c}$	$(\epsilon_{abc} Q_a^T C \gamma_\mu Q_b Q_c)(Q_e \gamma_\rho \bar{Q}_e)$	$\frac{5}{2}^-$	$7.76_{-0.18}^{+0.23}$			
$bbbb\bar{b}$	$(\epsilon_{abc} Q_a^T C \gamma_\mu Q_b Q_c)(Q_e \gamma_\rho \bar{Q}_e)$	$\frac{5}{2}^-$	$22.27_{-0.22}^{+0.22}$			
$cccc\bar{c}$	$(\epsilon_{abc} Q_a^T C \gamma_\mu Q_b Q_c)(Q_e \gamma_\rho \gamma_5 \bar{Q}_e)$	$\frac{5}{2}^+$	$7.81_{-0.18}^{+0.17}$			
$bbbb\bar{b}$	$(\epsilon_{abc} Q_a^T C \gamma_\mu Q_b Q_c)(Q_e \gamma_\rho \gamma_5 \bar{Q}_e)$	$\frac{5}{2}^+$	$22.37_{-0.20}^{+0.18}$			

provided that they allow strong decay processes to occur. Among them, the states with $J^P = \frac{3}{2}^+$ could be detected in the $\Omega_{QQQ}\chi_{Q0}$ invariant mass spectrum, the states with $J^P = \frac{5}{2}^-$ in the $\Omega_{ccc}J/\psi$ and $\Omega_{bbb}\Upsilon$ invariant mass spectrum, and the states with $J^P = \frac{5}{2}^+$ in the $\Omega_{QQQ}\chi_{Q1}$ invariant mass spectrum, respectively. Anyhow, subsequent theoretical studies and intensive experimental observations will provide an important basis for revealing the nature of these peculiar fully heavy pentaquark states.

Acknowledgments

This work was supported by the National Natural Science Foundation of China under Contract No. 11475258. The authors are very grateful to Xiang Liu for recent communication and helpful discussion.

-
- [1] H. X. Chen, W. Chen, X. Liu, and S. L. Zhu, Phys. Rep. **639**, 1 (2016).
 - [2] H. X. Chen, W. Chen, X. Liu, Y. R. Liu, and S. L. Zhu, Rept. Prog. Phys. **80**, 076201 (2017).
 - [3] A. Esposito, A. Pilloni, and A. Polosa, Phys. Rep. **668**, 1 (2017).
 - [4] A. Ali, J. S. Lange, and S. Stone, Prog. Part. Nucl. Phys. **97**, 123 (2017).
 - [5] F. K. Guo, C. Hanhart, U. G. Meissner, Q. Wang, Q. Zhao, and B. S. Zou, Rev. Mod. Phys. **90**, 015004 (2018).
 - [6] Y. R. Liu, H. X. Chen, W. Chen, X. Liu, and S. L. Zhu, Prog. Part. Nucl. Phys. **107**, 237 (2019).
 - [7] N. Brambilla, S. Eidelman, C. Hanhart, A. Nefediev, C. P. Shen, C. E. Thomas, A. Vairo, and C. Z. Yuan, Phys. Rep. **873**, 1 (2020).
 - [8] G. Yang, J. L. Ping, and J. Segovia, Symmetry **12** (2020).
 - [9] H. X. Chen, W. Chen, X. Liu, Y. R. Liu, and S. L. Zhu, Rept. Prog. Phys. **86**, 026201 (2023).
 - [10] S. K. Choi *et al.* (Belle Collaboration), Phys. Rev. Lett. **91**, 262001 (2003).
 - [11] R. Aaij *et al.* (LHCb Collaboration), Phys. Rev. Lett. **115**, 072001 (2015).
 - [12] R. Aaij *et al.* (LHCb collaboration), Phys. Rev. Lett. **122**, 222001 (2019).
 - [13] R. Aaij *et al.* (LHCb collaboration), Sci. Bull. **66**, 1278 (2021).
 - [14] R. Aaij *et al.* (LHCb Collaboration), Phys. Rev. Lett. **131**, 031901 (2023).
 - [15] R. Aaij *et al.* (LHCb Collaboration), Phys. Rev. Lett. **128**, 062001 (2022).
 - [16] R. Aaij *et al.* (LHCb Collaboration), Sci Bull **65**, 1983 (2020).

- [17] H. T. An, K. Chen, Z. W. Liu, and X. Liu, Phys. Rev. D **103**, 074006 (2021).
- [18] J. R. Zhang, Phys. Rev. D **103**, 074016 (2021).
- [19] Z. G. Wang, Nucl. Phys. B **973**, 115579 (2021).
- [20] Y. Yan, Y. Wu, X. Hu, H. Huang, and J. Ping, Phys. Rev. D **105**, 014027 (2022).
- [21] H. T. An, S. Q. Luo, Z. W. Liu, and X. Liu, Phys. Rev. D **105**, 074032 (2022).
- [22] G. Yang, J. Ping, and J. Segovia, Phys. Rev. D **106**, 014005 (2022).
- [23] W. X. Zhang, H. T. An, and D. Jia, Eur. Phys. J. C **83**, 727 (2023).
- [24] Y. Yan, Y. Wu, H. Huang, J. Ping, and X. Zhu, Eur. Phys. J. C **83**, 610 (2023).
- [25] Z. B. Liang, F. X. Liu, and X. H. Zhong, Phys. Rev. D **111**, 056013 (2025).
- [26] K. Azizi, Y. Sarac, and H. Sundu, Eur. Phys. J. C **84**, 695 (2024).
- [27] M. C. Gordillo, J. Segovia, and J. M. Alcaraz Pelegrina, Phys. Rev. D **110**, 094024 (2024).
- [28] K. Azizi, Y. Sarac, and H. Sundu, arXiv:2502.09409 [hep-ph].
- [29] R. Farashaeian and S. M. M. Nejad, Eur. Phys. J. A **60**, 65 (2024).
- [30] A. Sharma and A. Upadhyay, arXiv:2504.04546 [hep-ph].
- [31] H. Song, X. R. Liu, J. Q. Xie, and J. K. Chen, arXiv:2506.01005 [hep-ph].
- [32] M. A. Shifman, A. I. Vainshtein, and V. I. Zakharov, Nucl. Phys. B **147**, 448 (1979).
- [33] M. A. Shifman, A. I. Vainshtein, and V. I. Zakharov, Nucl. Phys. B **147**, 385 (1979).
- [34] B. L. Ioffe, in The Spin Structure of the Nucleon, edited by B. Frois, V. W. Hughes, and N. de Groot (World Scientific, Singapore, 1997).
- [35] S. Narison, Camb. Monogr. Part. Phys. Nucl. Phys. Cosmol. **17**,1 (2002), arXiv:hep-ph/0205006.
- [36] P. Colangelo and A. Khodjamirian, in At the Frontier of Particle Physics: Handbook of QCD, Vol. 3, edited by M. Shifman and B. I. Festschrifts (World Scientific, Singapore, 2001) pp. 1495–1576.
- [37] M. Nielsen, F. S. Navarra, and S. H. Lee, Phys. Rep. **497**, 41 (2010).
- [38] Z. G. Wang, arXiv:2502.11351 [hep-ph].
- [39] L. Reinders, H. Rubinstein, and S. Yazaki, Phys. Rep. **127**, 1 (1985).
- [40] E. Shuryak, Nucl. Phys. B **198**, 83 (1982).
- [41] B. Ioffe, Nucl. Phys. B **188**, 317 (1981).
- [42] H. Kim and Y. Oh, Phys. Rev. D **72**, 074012 (2005).
- [43] M. Bracco, A. Lozea, R. Matheus, F. Navarra, and M. Nielsen, Phys. Lett. B **624**, 217 (2005).
- [44] R. D. Matheus, S. Narison, M. Nielsen, and J. M. Richard, Phys. Rev. D **75**, 014005 (2007).
- [45] J. R. Zhang and M. Q. Huang, Phys. Lett. B **674**, 28 (2009).
- [46] J. R. Zhang, Phys. Rev. D **87**, 076008 (2013).
- [47] J. R. Zhang, Phys. Rev. D **89**, 096006 (2014).
- [48] J. R. Zhang, Phys. Rev. D **103**, 014018 (2021).
- [49] M. Nielsen, F. S. Navarra, and S. H. Lee, Phys. Rep. **497**, 41 (2010).
- [50] V. A. Novikov, M. A. Shifman, A. I. Vainshtein, and V. I. Zakharov, Fortschr. Phys. **32**, 585 (1984).
- [51] G. Launer, S. Narison, and R. Tarrach, Z. Phys. C **26**, 433 (1984).
- [52] S. Narison, Phys. Lett. B **673**, 30 (2009).
- [53] S. Narison, Phys. Rep. **84**, 263 (1982).
- [54] S. Navas *et al.* (Particle Data Group), Phys. Rev. D **110**, 030001 (2024).